SOI ring resonators with controllable MMI coupler sections

Youfang Hu, Frédéric Gardes, Goran Mashanovich, Graham Reed

Youfang Hu, Frédéric Y. Gardes, Goran Z. Mashanovich, Graham T. Reed, "SOI ring resonators with controllable MMI coupler sections," Proc. SPIE 7943, Silicon Photonics VI, 794311 (17 January 2011); doi: 10.1117/12.887692

SPIE.

Event: SPIE OPTO, 2011, San Francisco, California, United States

SOI ring resonators with controllable MMI coupler sections

Youfang Hu*, Frédéric Y. Gardes, Goran Z. Mashanovich, Graham T. Reed
Advanced Technology Institute, University of Surrey, Guildford, GU2 7XH, UK

ABSTRACT

A ring resonator using a single 2×2 MMI as the coupler section has the distinct advantages of low sensitivity to fabrication error, temperature, wavelength and polarisation. However, the coupling coefficient of the 2×2 MMI coupler is fixed; hence, the performance of this type of device is limited, e.g. transmission spectrum with high extinction ratio is difficult to achieve. We have designed and simulated ring resonators with coupler sections consisting of two 2×2 MMIs and phase shifters, so that the coupling efficiency can be varied from 0% to 100% with relative ease. For a single ring resonator, the transmission spectrum can be controlled to achieve an extinction ratio of >20dB and a spectral bandwidth of <1nm. For a multiple ring filter, the transmission spectrum can be controlled to achieve an extinction ratio of >30dB and a bandwidth of <1nm; in addition, a flat-top transmission spectrum is also achievable. The whole device has a footprint of approximately 200μm by 100μm.

Keywords: ring resonators, SOI, multimode interferometer, coupler, temperature control

1. INTRODUCTION

The use of 2×2 multimode interferometers (MMIs) as the coupling section in SOI ring resonators provides several distinct advantages over those using directional couplers, such as low wavelength sensitivity, low polarisation sensitivity, and low fabrication tolerance sensitivity[1-4]. However, this type of device has its own limitation because the power splitting ratio of a single 2×2 MMI is fixed at either 0.5:0.5 for type I and type II MMIs or 0.15:0.85 for type III MMIs[1]. Specific performance of such ring resonators, e.g. transmission spectrum with high extinction ratio is consequentially difficult to achieve. Here, we reported a design of an SOI ring resonator using two 2×2 MMIs and one phase shifter as the coupler section. The power splitting ratio can be continuously varied from 1:0 to 0:1 with moderate temperature control. Hence, a number of interesting features can be achieved, e.g. variable extinction ratio, and flat-top spectral response at drop port.

2. DESIGN OF CONTROLLABLE MMI COUPLER SECTION

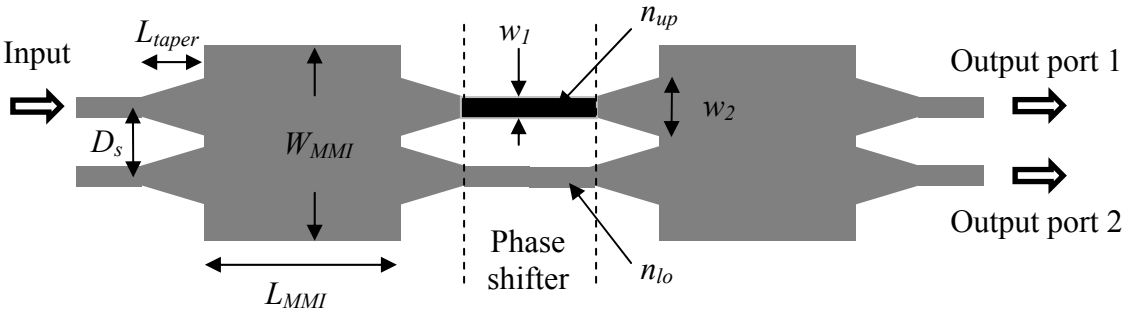

Fig. 1 Design of controllable MMI coupler section (top view)

*email: y.hu@surrey.ac.uk; phone: +44 1483 68 9831

Silicon Photonics VI, edited by Joel A. Kubby, Graham T. Reed, Proc. of SPIE Vol. 7943,
794311 · © 2011 SPIE · CCC code: 0277-786X/11/$18 · doi: 10.1117/12.887692

The structure of a controllable MMI coupler section is shown in Fig.1. It consists of two identical 2×2 MMIs with phase shifter interconnecting them. The 2×2 MMI is based on the design of a type II MMI shown in [1], with a power splitting ratio of 0.5:0.5. The MMI has a length of L_{MMI}=25μm and a width of W_{MMI}=4.5μm. The single mode accessing waveguides for input, output and phase shifter have the same width, w_1=0.4μm, and a centre to centre separation of D_s=1.6μm. These single-mode waveguides are linearly tapered to a width of w_2=1.5μm before connecting the multimode waveguides. The taper has a length of L_{taper}=3μm. The phase shifter is simply made of the two single-mode waveguides connecting the MMIs with one waveguide having variable effective index (the upper one shown in Fig.1). All the waveguides, both single-mode and multi-mode, are based on a SOI rib structure with an overlayer height of H=220nm, and a slab height of h=50nm, as is shown in Fig. 2.

These design parameters were firstly estimated by fitting the formula of the first order 3-dB coupling condition with 2-D approximation, given by:

$$W_{MMI} = 3D_s$$

$$L_{MMI} = \frac{2n_s W_{MMI}^2}{3\lambda}$$

where, n_s is the effective index of counterpart 2-D slab waveguide and λ is the operating wavelength. The parameters were then slightly adjusted by using a 3-D simulation tool FIMMWAVE[5] to optimise the transmission efficiency of the MMI.

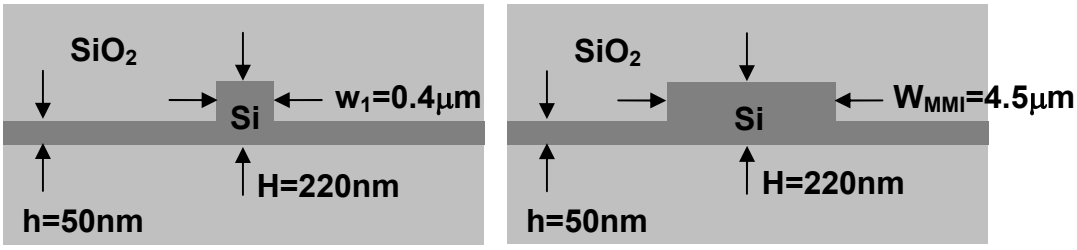

(a) (b)

Fig.2 (a) single-mode waveguide and (b) multi-mode waveguide of MMI

Assuming the input signal is launched from the upper left waveguide, shown in Fig. 1, we are able to continuously vary the power splitting ratio of the two output ports by changing the effective index of one single mode waveguide in the phase shifter. First, the input power is evenly coupled into the two output ports of the first MMI. The two input waveguides of the second MMI will receive a signal with the same power level but different phase delay. The signal will eventually be coupled into the two output waveguides at different ratios depending on the phase delay.

Fig. 3 shows the transmittivity of the two output ports as a function of the effective index of the upper single mode waveguide in the phase shifter, n_{up}, assuming a phase shifter length of L_{ps}=20μm. This shows that a continuous change of output coupling ratio from 0:1 to 1:0 requires refractive index change of $\Delta n_\pi = 3.6\times10^{-2}$ (half-period width in Fig. 3). Since the phase delay is linearly dependant on phase shifter's length, a phase shifter length of L_{ps}=200μm will only require $\Delta n_\pi = 3.6\times10^{-3}$, which is achievable by a temperature change within the range of 20°C for SOI single-mode waveguides shown in Fig. 2(a).

Fig. 4 shows the field profiles of the whole coupler at power splitting ratios of 0:1, 0.5:0.5 and 1:0 for different n_{up}.

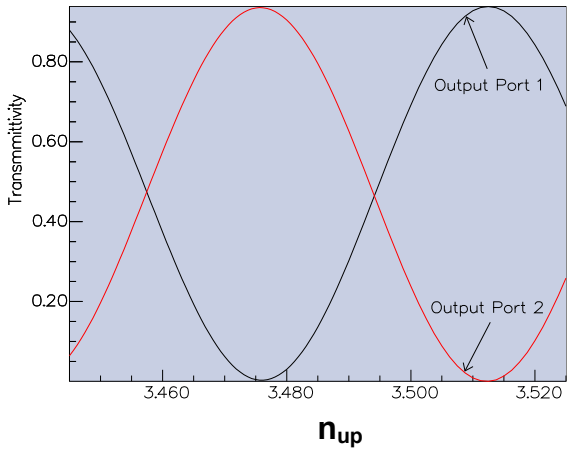

Fig. 3 Coupler transmittivity vs n_{up} (L_{ps}=20μm, n_{lo}=3.476)

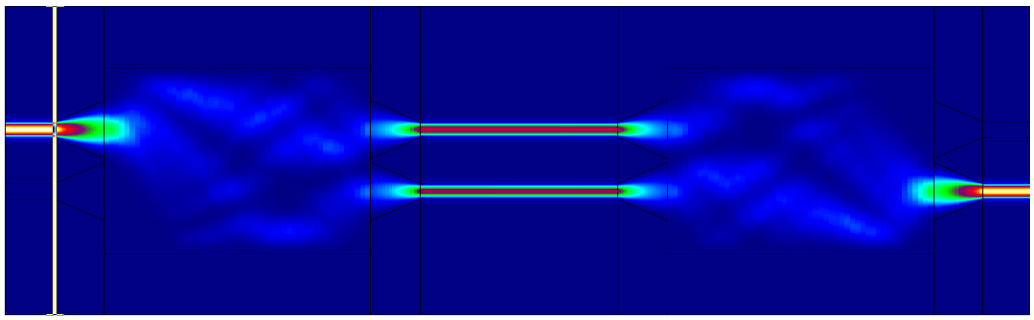

(a) Output power splitting ratio 0:1, n_{up} = 3.476, n_{lo}=3.476

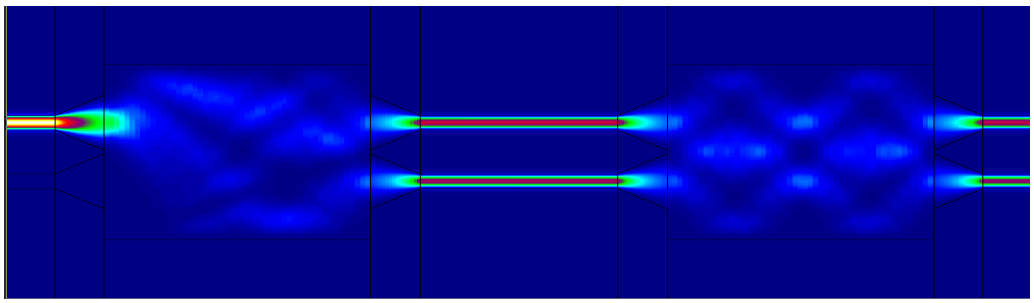

(b) Output power splitting ratio 0.5:0.5, n_{up} = 3.493, n_{lo}=3.476

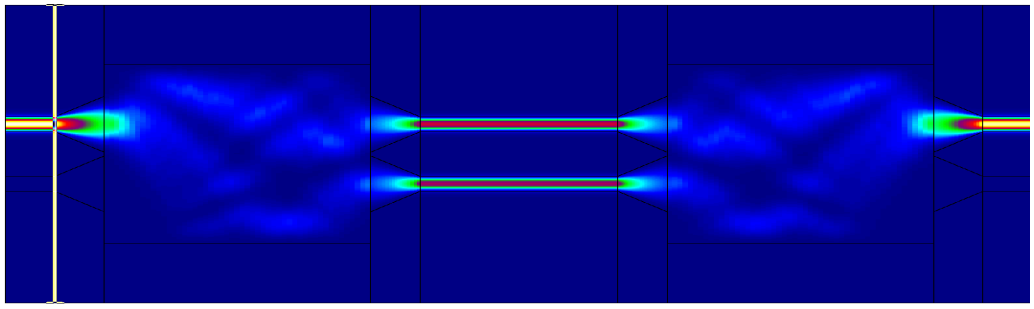

(c) Output power splitting ratio 1:0, n_{up} = 3.512, n_{lo}=3.476

Fig. 4 Field profiles of the coupler at different power splitting ratios

3. DESIGN OF RING RESONATOR

Fig. 5 shows the design of single and double ring resonators with controllable MMI coupler sections. The phase shifter section in the coupler has two winding arms, which are symmetric in geometry and have a temperature controllable area (shown in shaded area in Fig. 5) on one arm of each coupler. As discussed in the previous section, the arm length of phase shifter should be long enough (>200μm) for a temperature control in the range of 20°C, hence, the bending radius, R, of the winding arms need to be optimised to make the whole device fit in as small footprint as possible and to keep the bending loss insignificant. Here, we have carried out the bending loss study using FIMMWAVE, as shown in Fig. 6, and found that R=5μm is a practical design value. This results in a single ring resonator design covering an area of $100\times100\mu m^2$ and a double ring resonator covering an area of $155\times100\mu m^2$.

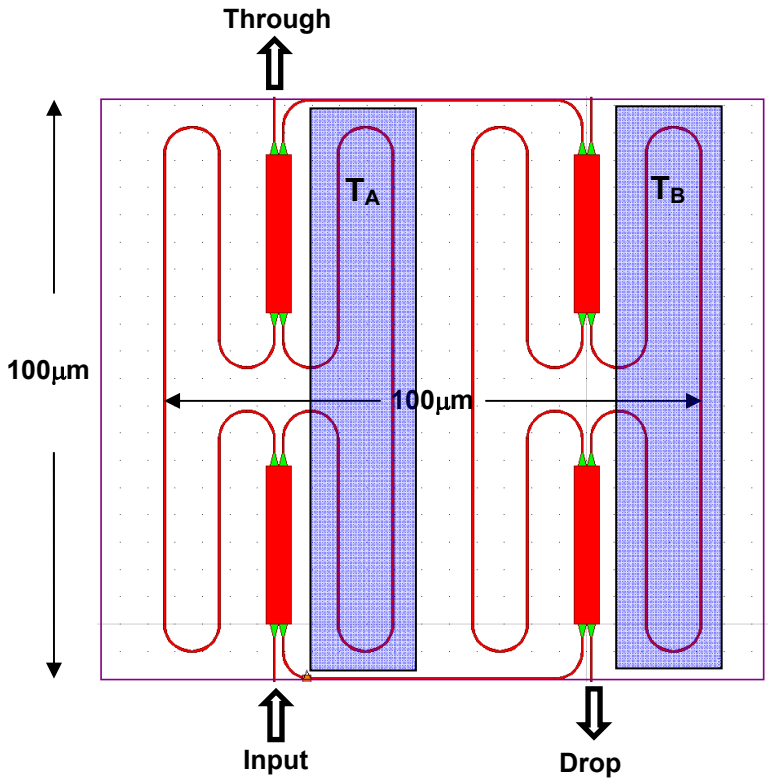

(a)

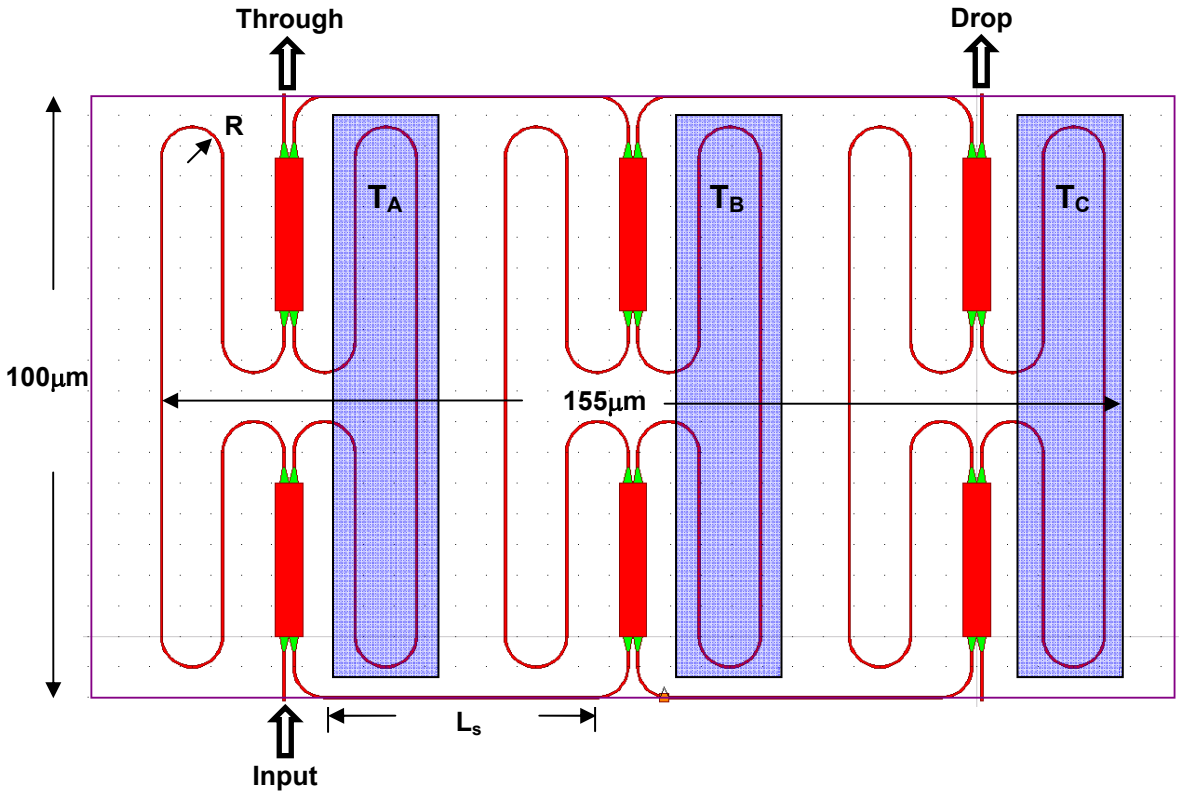

(b)

Fig.5 Layout for the design of (a) single ring resonator (b) double ring resonator

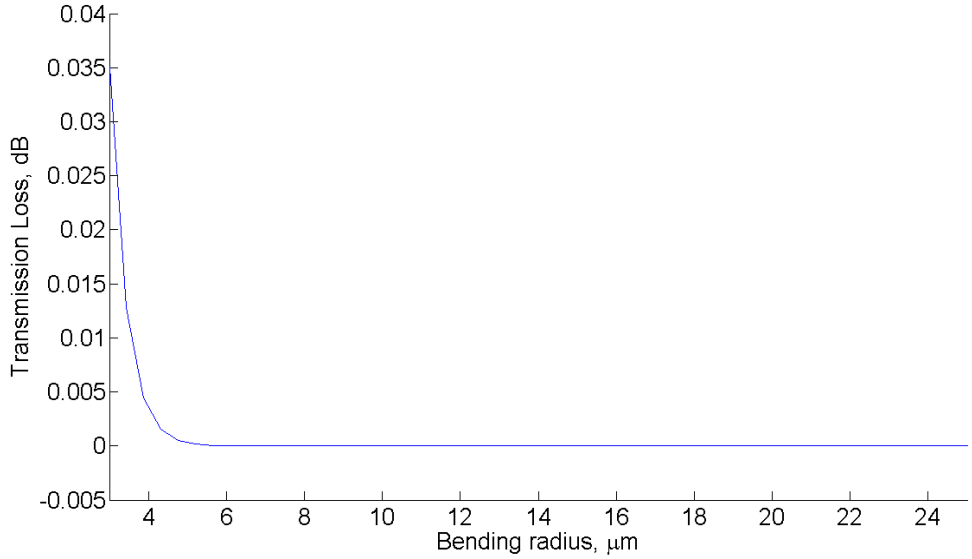

Fig. 6 Simulation result (FIMMWAVE) of 90° bending loss for the single-mode waveguide shown in Fig. 2(a)

An analytical model based on transfer matrix method (TMM) was developed for the modelling of the above devices. The transfer matrix for the whole coupler is defined by:

$$M_c = M_{MMI} M_{ps} M_{MMI}$$

where, M_{MMI}, is the transmission matrix of a single 2×2 MMI using the design parameters and simulation result given in section 2. M_{ps} is the transfer matrix of phase shifter, which is defined by:

$$M_{ps} = \begin{bmatrix} \exp(i\beta_0 L_{ps}) & 0 \\ 0 & \exp(i\beta_1 L_{ps}) \end{bmatrix}$$

where, β_0 is the propagation constant of the single-mode waveguide with fixed effective index in the phase shifter, and β_1 is the propagation constant of the single-mode waveguide with variable effective index in the phase shifter, L_{ps} is the length of the single mode waveguide in the phase shifter section.

The transmission matrix of the waveguide sections connecting two couplers is given by:

$$N_{ccw} = \begin{bmatrix} \exp(i\beta_0 L_s & 0 \\ 0 & \exp(-i\beta_0 L_s) \end{bmatrix}$$

for counter-clockwise propagating waves, or

$$N_{cw} = \begin{bmatrix} \exp(-i\beta_0 L_s & 0 \\ 0 & \exp(i\beta_0 L_s) \end{bmatrix}$$

for clockwise propagating waves.

L_s is the length of the waveguide connecting neighbouring coupler sections, shown in Fig. 5.

With some simple algebra, the whole transfer matrix of the single ring resonator, M_{SRR}, is given by:

$$M_{SRR} = M_c' N_{cw} M_c''$$

and that of the double ring resonator, M_{DRR}, is given by:

$$M_{DRR} = M_c' N_{cw} M_c'' N_{ccw} M_c'$$

where,

$$M_c' = \begin{bmatrix} \dfrac{M_c(2,2)}{M_c(1,2)} & M(2,1) - \dfrac{M_c(1,1)M_c(2,2)}{M_c(1,2)} \\ \dfrac{1}{M_c(1,2)} & -\dfrac{M_c(1,1)}{M_c(1,2)} \end{bmatrix}$$

$$M_c'' = \begin{bmatrix} -\dfrac{M_c(1,1)}{M_c(1,2)} & \dfrac{1}{M_c(1,2)} \\ M(2,1) - \dfrac{M_c(1,1)M_c(2,2)}{M_c(1,2)} & \dfrac{M_c(2,2)}{M_c(1,2)} \end{bmatrix}.$$

Now we have single ring resonator's drop port response given by:

$$T_{drop}^{SRR} = M_{RR}(2,2) - \frac{M_{RR}(1,2)M_{RR}(2,1)}{M_{RR}(1,1)},$$

double ring resonator's drop port response given by

$$T_{drop}^{DRR} = M_{RR}(1,2) - \frac{M_{RR}(1,1)M_{RR}(2,2)}{M_{RR}(2,1)},$$

single ring resonator's through port response given by:

$$T_{through}^{SRR} = -\frac{M_{RR}(1,2)}{M_{RR}(1,1)},$$

and double ring resonator's through port response given by

$$T_{through}^{DRR} = -\frac{M_{RR}(2,2)}{M_{RR}(2,1)}.$$

4. SIMULATION RESULTS

The simulation results of the spectral response for the single ring resonator are shown in Fig. 7. The device has a background temperature of T_{bg}=20°C. Without local temperature control, i.e. T_A=T_B=T_{bg}=20°C, both couplers in the single ring resonator have a power splitting ratio of 0.5:0.5. The drop port's spectrum has an extinction ratio of ~25dB, and the through port has an extinction ratio of ~5dB (Fig. 7a). In order to maximise the extinction ratio of the ring resonator's spectral response, we keep T_A=T_B, where the power splitting ratio of the two couplers are the same. In our simulation, T_A and T_B vary from 5°C to 40°C, the largest extinction ratio from through port, 30dB, appears at T_A=T_B=5°C (Fig. 7b), and the largest extinction ratio from drop port, 30dB, appears at T_A=T_B=25°C (Fig. 7c). However, there is a trade-off between extinction ratio and insertion loss for the spectral response. If insertion loss is to be kept to a minimum for both through and drop ports, the ring resonator has an extinction ratio of 15dB from the through port and 20dB from the drop port at T_A=T_B=30°C (Fig. 7d).

The simulation results of the spectral response for the double ring resonator are shown in Fig. 8. The device's background temperature is also kept at T_{bg}=20°C, Without local temperature control, i.e. T_A=T_B=T_{bg}=20°C, all the three couplers have a power splitting ratio of 0.5:0.5, the spectral response from drop port has a double peak and the extinction ratio is about 40dB. However, with local temperature control, the drop port has flat-top spectrum feature with negligible insertion loss at T_A=T_C=10°C, T_B=15°C, with a -3dB bandwidth of 0.3nm and an extinction ratio of 18dB (Fig. 8b). A flat-top response with a larger extinction ratio can be found at T_A=T_C=15°C, T_B=20°C (32dB) (Fig. 8c), and T_A=T_C=20°C, T_B=25°C (50dB) (Fig. 8d), however, the -3dB bandwidth is smaller and the insertion loss is higher.

The free spectral range (FSR), Δλ, in our design can be expressed as:

$$\Delta\lambda = \frac{\lambda_r^2}{L_c n_g}$$

where, λ_r is the resonant wavelength, L_c is the circumference of the ring, and n_g is group refractive index at resonant wavelength. The FSR in our design is limited to be <1nm due to the long single-mode waveguides (L_{ps}=200μm) used in the phase shifter section, which is a part of the ring's circumference (L_c). L_{ps} must be long enough so that moderate

change (-20°C<ΔT<20°C) of local temperatures (T_A, T_B, T_C shown in Fig. 5) can give enough phase delay in the phase shifter sections, hence, effective control of the coupler's power splitting ratio. Nevertheless, it is possible to design high-order ring resonators with the Vernier effect, where larger FSR is achievable.

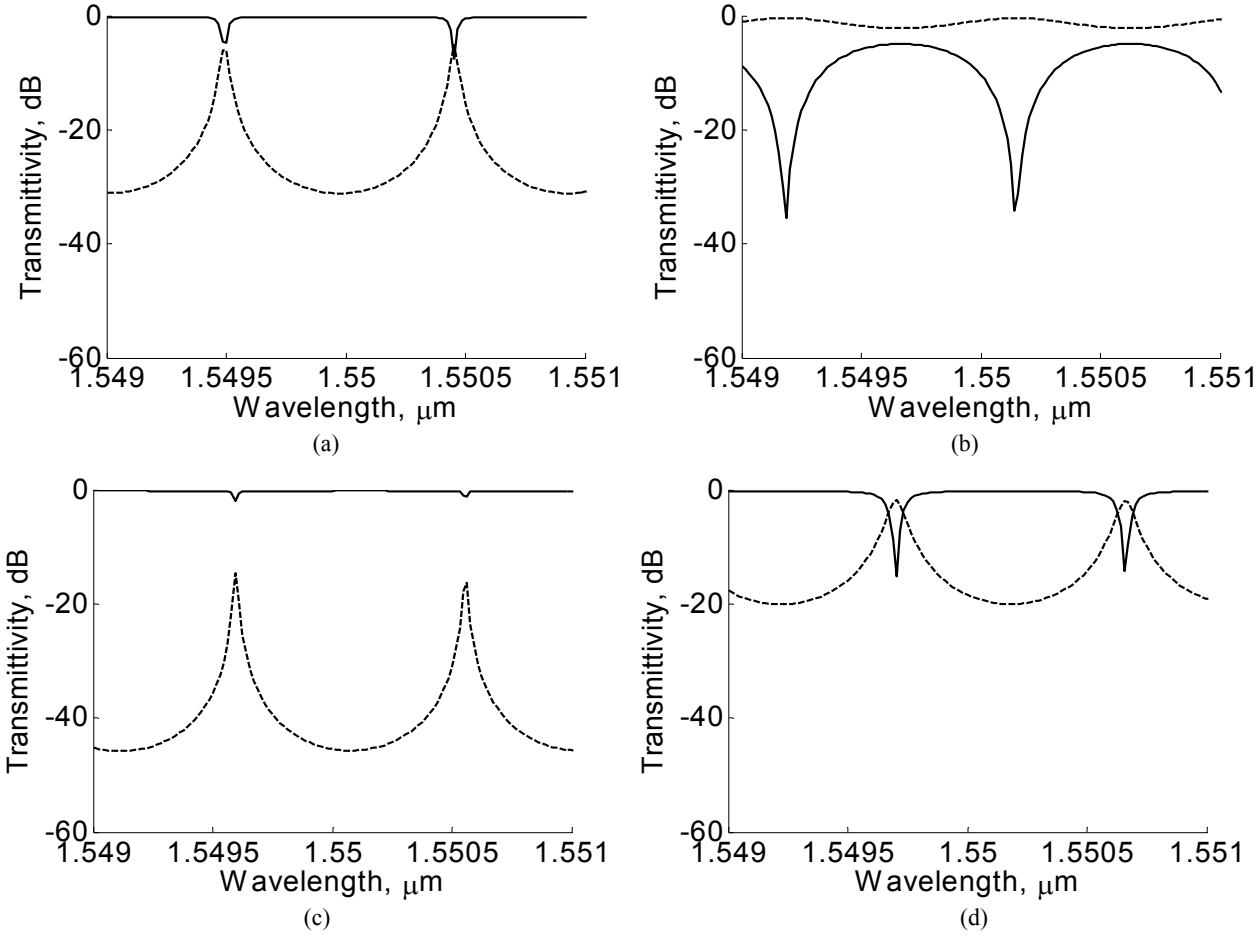

Fig. 7. Simulation of spectrum response of single ring resonator from through port (solid line) and drop port (dashed line) at (a) T_A=T_B=20°C, (b) T_A=T_B=5°C, (c) T_A=T_B=25°C, and (d) T_A=T_B=30°C. Background temperature: T_{bg}=20°C.

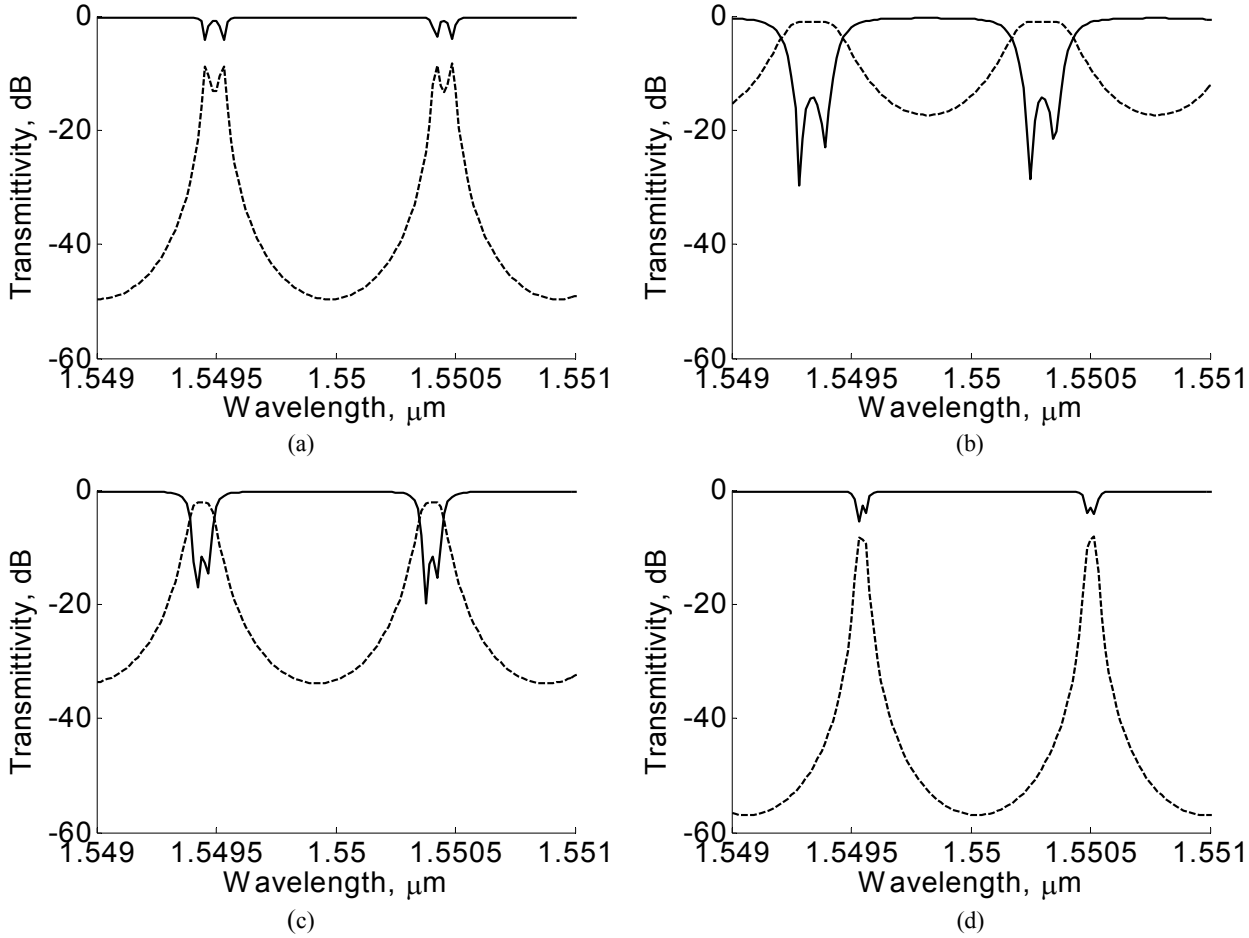

Fig. 8. Simulation of spectrum response of double ring resonator from through port (solid line) and drop port (dashed line) at (a) T_A=T_C=T_B=20°C; (b) T_A=T_C=10°C, T_B=15°C; (c) T_A=T_C=15°C, T_B=20°C; (d) T_A=T_C=20°C, T_B=25°C. Background temperature: T_{bg}=20°C.

5. CONCLUSION

In conclusion, ring resonators with controllable MMI coupler sections were designed and simulated. The coupler section consists of two identical MMIs connected by a phase shifter such that its power splitting ratio is controllable by varying the phase delay in the phase shifter section. The phase delay is achieved by moderate local temperature change of one arm in the phase shifter section. Simulation shows that controllable extinction ratio and insertion loss are achievable for both single and double ring resonators. In addition, with specific local temperature control, flat top spectrum feature can be obtained at the double ring resonator's drop port. The free spectral range of the ring resonator is about 1nm. There is a potential to design similar controllable multiple ring resonators via the Vernier effect to achieve larger free spectral range.

REFERENCES

[1] M. K. Chin, C. L. Xu, and W. P. Huang, "Theoretical approach to a polarization insensitive single-mode microring resonator," Optics Express, 12(14), 3245-3250 (2004).

[2] D. X. Xu, S. Janz, and P. Cheben, "Design of polarization-insensitive ring resonators in Silicon-on-Insulator using MMI couplers and cladding stress engineering," IEEE Photonics Technology Letters, 18(2), 343-345 (2006).

[3] D. X. Xu, A. Densmore, P. Waldron, J. Lapointe, E. Post, A. Delâge, S. Janz, P. Cheben, J. H. Schmid, and B. Lamontagne, "High bandwidth SOI photonic wire ring resonators using MMI couplers," Optics Express, 15(6), 3149-3155 (2007).

[4] D. J. Thomson, Y. Hu, G. T. Reed, Jean-Marc Fedeli, "Low Loss MMI Couplers for High Performance MZI Modulators," IEEE Photonics Technology Letters, 22(20), 1485-1487 (2010).

[5] http://www.photond.com.